Measurement of the residual stress in chromium nitride coatings deposited on an aluminum alloy substrate using arc ion plating method

Kazuya Kusaka,[1,a)] Kenta Shirasaka,[2] Daisuke Yonekura,[1] and Yuta Tanaka[3]
[1]*Institute of Technology and Science, Tokushima University, 2-1, Minamijosanjima, Tokushima, Tokushima 7708506, Japan*
[2]*Graduate School of Advanced Technology and Science, Tokushima University, 2-1, Minamijosanjima, Tokushima, Tokushima 7708506, Japan*
[3]*Materials Department, Research Laboratory, IHI Corporation, 1, Shin-nakahara-cho, Isogo-ku, Yokohama, Kanagawa 235-8501, Japan*

(Received 4 July 2019; accepted 8 October 2019; published 28 October 2019)

Chromium nitride (CrN) coatings were deposited on Al alloy substrates using the arc ion plating method with different bias voltages and different thicknesses. The residual stresses of these samples were measured via x-ray diffraction using the $\sin^2\psi$ method because the CrN crystals in the coatings were nonoriented. The stress gradient across the CrN coating was calculated from the curved 2θ-$\sin^2\psi$ diagram. In the case of CrN coatings deposited at low bias voltage, the compressive residual stress that formed at the substrate interface was larger than the stress at the surface of the CrN coating. Conversely, in the case of CrN coatings deposited at high bias voltage, the compressive residual stress on the surface of the CrN coating was larger than the stress on the interface with the substrate. In CrN coatings deposited at high bias voltage, very large compressive residual stress on the CrN coating surface decreased with increasing coating thickness. *Published by the AVS.*
https://doi.org/10.1116/1.5118702

I. INTRODUCTION

Chromium nitride (CrN) coatings prepared via physical vapor deposition (PVD) have greater heat resistance than coatings deposited via electroplating. Because these coatings are very hard and exhibit a sliding property, they are used as a protective coating for cutting tools,[1,2] die-castings,[3] and as a coating for piston rings and connecting rods in automobile engines.[4,5]

Residual stresses always develop in such coatings, because the coating and the substrate differ in atomic spacing, coefficients of thermal expansion, and cooling conditions. Significant residual stress may cause microcracks in the coating or cause the coating to peel from the substrate. When a hard coating is deposited on a soft substrate via PVD, a complicated stress distribution is formed in the hard coating. Therefore, controlling the residual stress is important for synthesizing mechanically stable CrN coatings.

It is difficult to form a hard coating on a soft substrate. A large residual stress is formed in the hard film deposited by the arc ion plating (AIP) method, and the soft substrate surface undergoes plastic deformation without being able to withstand it. As a result, it is considered that a complex residual stress distribution is formed in the hard film. In this study, we measured the residual stress in hard CrN coatings deposited on a soft aluminum alloy substrate under various conditions. Additionally, we investigated the stress gradient formed in the CrN coatings by observing the curvature of the $\sin^2\psi$ diagram.

II. EXPERIMENT

A. Coating preparation

CrN coatings were prepared using an AIP system. The substrate material was an Mg-based aluminum alloy (JIS: A5083) in the form of $25 \times 25 \times 5\ \mathrm{mm}^3$ plates.

The substrate was bombarded with accelerated energetic ions created by an arc discharge near a chromium target for 0.8 min; as a result, the surface of the substrate was cleaned by etching with Cr ions. After cleaning, the CrN coatings were deposited under the conditions described in Table I.

B. X-ray stress analysis of CrN coatings

CrN powder has a face-centered cubic structure with lattice parameters of $a = 0.415$ nm.[6] The CrN coatings deposited on the aluminum alloy substrate using the AIP method had a mixed crystal structure that was both random oriented and {110}-oriented. A diffraction peak from the CrN crystals was obtained at every ψ angle, and so the $\sin^2\psi$ method[7] was used for residual stress measurements.

The residual stress in these CrN coatings was measured via x-ray diffraction using CuKα characteristic x-rays. The residual stress was calculated for the 311 diffraction peak at $2\theta = 76.2°$ using the following equation:[7]

$$\sigma = \frac{E_X}{1+\nu_X}\frac{\partial\,\varepsilon_\psi}{\partial \sin^2\psi}, \tag{1}$$

where E_X and ν_X are the diffraction elastic constant and Poisson's ratio of CrN, respectively, and ψ is the angle between the normal axis of the diffraction plane and the normal axis of the surface. The values of E_X and ν_X were calculated via the Kröner model analysis[8] using the elastic stiffness values, c_{ij}, of

Note: This paper is part of the Conference Collection: 15th International Symposium on Sputtering and Plasma Processes (ISSP2019).
a)Electronic mail: kusaka@tokushima-u.ac.jp

TABLE I. Conditions of CrN deposition.

Arc current I_A (A)	70	70
Bias voltage V_B (V)	−60	−150
Heating temperature (K)	403	403
N_2 gas pressure (Pa)	5.33	5.33
Coating thickness t (μm)	2, 5	0.5, 1, 2, 3, 5
Revolution of table (rpm)	3	3

single crystal CrN. Because the values of c_{ij} for a CrN crystal were $c_{11} = 542$ GPa, $c_{12} = 27$ GPa, and $c_{44} = 88$ GPa,[9] the values of E_X and ν_X for the 311 diffraction peak were calculated to be 349.22 GPa and 0.2070, respectively.

III. RESULTS AND DISCUSSION

A. Structural evaluation of the CrN coating

Figure 1 shows the diffraction patterns obtained from CrN coatings deposited on the aluminum alloy substrate at various coating thicknesses ranging 0.5–5.0 μm, at a high bias voltage of −150 V. The diffraction peaks connected by a dashed line represent the same index of the aluminum crystal. The diffraction peaks connected by a bold line represent the CrN-220 diffraction peak. All diffractions of the aluminum crystal and the CrN crystals were observed, despite the smaller diffraction intensity of the CrN diffractions than that from aluminum. The intensity of the CrN-220 diffraction peak increased sharply with increasing coating thickness. The intensity ratio between the CrN-220 and the CrN-111 diffraction peaks was about 4.5 at $t = 3.0\,\mu$m and about 7.9 at $t = 5.0\,\mu$m. In the case of the CrN powder diffraction peak, which has a random oriented crystal structure, the diffraction intensity of CrN-220 was almost equal to that of CrN-111. From these results, it was found that the Al substrate has a random crystalline texture and the CrN coating deposited at high V_B has a mixed structure of random and {110}-oriented crystalline texture.

Figure 2 shows the diffraction pattern taken from CrN coatings deposited on the aluminum alloy substrate with a coating thickness of 5.0 μm at a low bias voltage of −60 V. The intensity ratio between the CrN-220 and CrN-111 diffraction peaks was about 1.0. The other diffraction intensity ratios were almost the same as those obtained via powder diffraction.

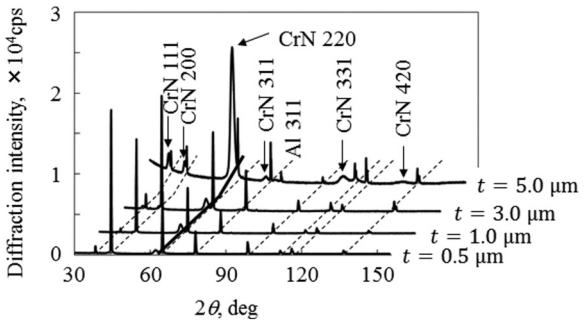

FIG. 1. Diffraction patterns of the CrN coatings deposited on aluminum alloy at $V_B = -150$ V.

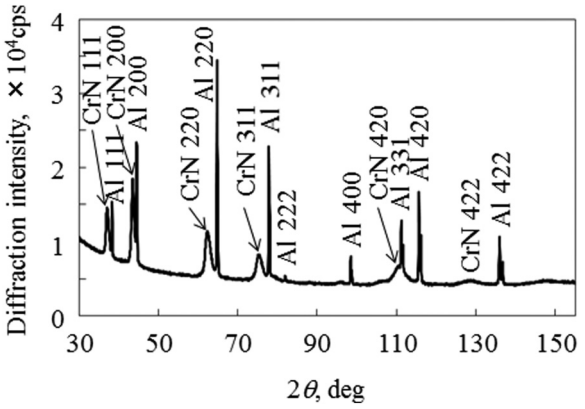

FIG. 2. Diffraction pattern of the CrN coatings deposited on aluminum alloy at $V_B = -60$ V and $t = 5.0\,\mu$m.

Therefore, we conclude that the CrN coating deposited at low V_B has a crystal structure of random orientation.

B. Residual stress in the CrN coating

The residual stress was measured for the CrN-311 diffraction peak at around $2\theta = 76.2°$. Figure 3 shows the diffraction peak measured at $\psi = 0°$ and 56.8° for the coating deposited at $V_B = -150$ V, $t = 2\,\mu$m. There was a very large Al-311 diffraction peak near the CrN-311 peak. Additionally, the CrN-311 diffraction peak shifted toward a high 2θ angle with increasing ψ due to the large compressive residual stress in the CrN

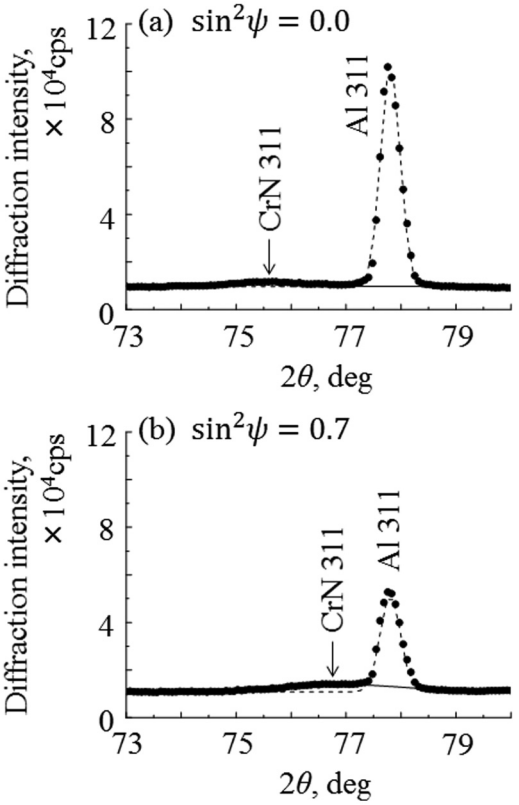

FIG. 3. CrN-311 and Al-311 diffraction patterns at $\sin^2\psi = 0$ and 0.7 of the coatings deposited at $V_B = -150$ V and $t = 2\,\mu$m.

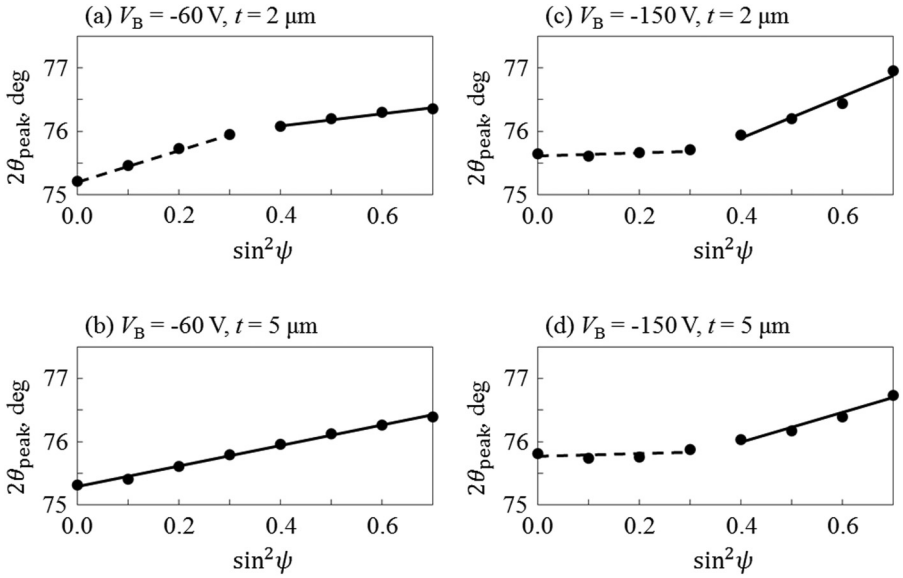

FIG. 4. 2θ-$\sin^2\psi$ diagrams of the CrN coatings. (a) $V_B = -60$ V, $t = 2\,\mu$m, (b) $V_B = -60$ V, $t = 5\,\mu$m, (c) $V_B = -150$ V, $t = 2\,\mu$m, and (d) $V_B = -150$ V, $t = 5\,\mu$m.

coating. In the above results, it was difficult to perform a background correction to determine the exact position of the CrN-311 diffraction peak. Therefore, we split the CrN-311 and the Al-311 diffraction peaks by simultaneously measuring them both and then performed a Gaussian multiple peak separation. With this method, it was possible to simultaneously measure the stresses in the CrN coating and the Al alloy substrate.

Figure 4 shows the experimental results of 2θ against $\sin^2\psi$ for CrN coatings deposited at (a) $V_B = -60$ V, $t = 2\,\mu$m, (b) $V_B = -60$ V, $t = 5\,\mu$m, (c) $V_B = -150$ V, $t = 2\,\mu$m, and (d) $V_B = -150$ V, $t = 5\,\mu$m. The residual stress of coatings deposited at $t = 0.5$ and $1.0\,\mu$m could not be measured because of the very small CrN-311 diffraction intensity. All of the $\sin^2\psi$ diagrams that could be measured were curved except for the coatings that were deposited at $V_B = -60$ V, $t = 5\,\mu$m. The $\sin^2\psi$ diagram is curved because of the triaxial stress state where the shear component of σ_{31} exists or where σ_{11} changes in the depth direction. As a result of measuring in the $-\psi$ direction, it became clear that there is a stress gradient with σ_{11} changing in the depth direction because the ψ split could not be confirmed.

The 2θ-$\sin^2\psi$ diagram for the coating deposited at $V_B = -60$ V and $t = 2\,\mu$m was an upward convex curve. This means that near the interface with the substrate, a very large compressive residual stress was formed that decreased on approaching the surface. Conversely, the 2θ-$\sin^2\psi$ diagram for the coating deposited at $V_B = -60$ V, $t = 5\,\mu$m was a straight line. As the coating thickness became large, the effect of the large compressive residual stress near the interface disappeared; therefore, the stress gradient disappeared within the x-ray penetration depth.

All 2θ-$\sin^2\psi$ diagrams for the coating deposited at a high bias voltage of $V_B = -150$ V were downward convex curves. This represents a very large compressive residual stress near the coating surface that decreased on approaching the interface with the substrate.

C. Analysis of the stress gradient in the CrN coating

The x-ray penetration depth (T) for each ψ angle was calculated using the following equation:

$$T = \frac{x}{2} \sin\theta_0 \times \cos\psi, \tag{2}$$

where x shows the thickness at which the intensity of the transmitted x ray is 1/e. The value of x could be represented by the reciprocal of the μ value obtained by the product of the mass absorption coefficient μ/ρ and the density ρ. When calculated using literature values,[10] the thickness x that CuKα line can penetrate for the CrN coating was derived as $5.513\,\mu$m. Table II shows the results of the calculated x-ray penetration depth for each ψ angle of the 311 diffraction peak. Measurement at the position where $\sin^2\psi = 0.0$ gives the average stress from the surface to a depth of $1.70\,\mu$m, whereas measurement at $\sin^2\psi = 0.7$ gives the average stress from the surface to a depth of $0.93\,\mu$m.

In consideration of the stress gradient in the CrN coating, the 2θ-$\sin^2\psi$ diagrams were divided into two regions and were linearly approximated (Fig. 4). The stress calculated from the slope of the broken straight line drawn between the measurement points of $\sin^2\psi$ from 0.0 to 0.3 represents the average residual stress from the surface to a depth of $1.7\,\mu$m. Conversely, the stress calculated from the slope of the solid straight line drawn between the measurement points of $\sin^2\psi$ from 0.4 to 0.7 represents the average residual stress

TABLE II. X-ray penetration depth of CrN coating for each ψ angle.

$\sin^2\psi$	0.0	0.1	0.2	0.3	0.4	0.5	0.6	0.7
ψ (deg)	0.0	18.4	26.6	33.2	39.2	45.0	50.8	56.8
Penetration depth (μm)	1.70	1.61	1.52	1.42	1.32	1.20	1.07	0.93

TABLE III. Results of residual stress measurement.

V_B (V)	t (μm)	Material	Residual stress
−60	2	Al	−4.3 ± 7.1 MPa
		CrN	Stress gradient
			−7.54 ± 0.02 GPa
			−2.92 ± 0.07 GPa
−60	5	Al	16.1 ± 8.4 MPa
		CrN	−5.22 ± 0.10 GPa
−150	2	Al	7.0 ± 9.9 MPa
		CrN	Stress gradient
			−1.35 ± 0.14 GPa
			−10.95 ± 0.32 GPa
−150	3	Al	−1.7 ± 1.3 MPa
		CrN	Stress gradient
			−1.27 ± 0.17 GPa
			−10.02 ± 0.42 GPa
−150	4	Al	−1.7 ± 1.3 MPa
		CrN	Stress gradient
			−2.80 ± 0.19 GPa
			−10.98 ± 0.38 GPa
−150	5	Al	−3.8 ± 2.9 MPa
		CrN	Stress gradient
			−0.64 ± 0.23 GPa
			−7.47 ± 0.23 GPa

from the surface to a depth of 1.3 μm. Table III summarizes the residual stress results in the CrN coatings and Al alloy substrate. If there was a stress gradient in the coating, it was indicated by two numbers. The upper part of the table shows the average stress value of the whole coating, and the lower part shows the average stress value from the surface to the depth of 1.3 μm. The residual stresses in the Al alloy substrate were almost zero, irrespective of the deposition conditions. Very large compressive residual stresses were formed in the CrN coating due to ion bombardment.[11,12] When comparing the values in the lower part of Table III, it was found that the compressive residual stress near the surface of the CrN coatings that had been deposited at high V_B became larger than that of CrN coatings that were deposited at a low V_B. In the case of the coatings deposited at high V_B, it is thought that Cr ions with high acceleration energies reached the substrate and formed a larger compressive residual stress in the coatings. Additionally, because the substrate was a soft metal, it is possible that the substrate was deformed and was unable to withstand the large compressive residual stress of the coating, and so stress relaxation of the coating occurred near the interface with the substrate.

Figure 5 shows SEM images of the surface of the 5 μm-thick CrN coating deposited at (a) $V_B = -60$ V and (b) $V_B = -150$ V. The surface of the CrN coating deposited at $V_B = -60$ V had more droplets and craters compared to those deposited at $V_B = -150$ V. Therefore, it was considered that the residual stress near the surface of the CrN coatings deposited at $V_B = -60$ V became smaller than that at $V_B = 150$ V due to the presence of many craters. There

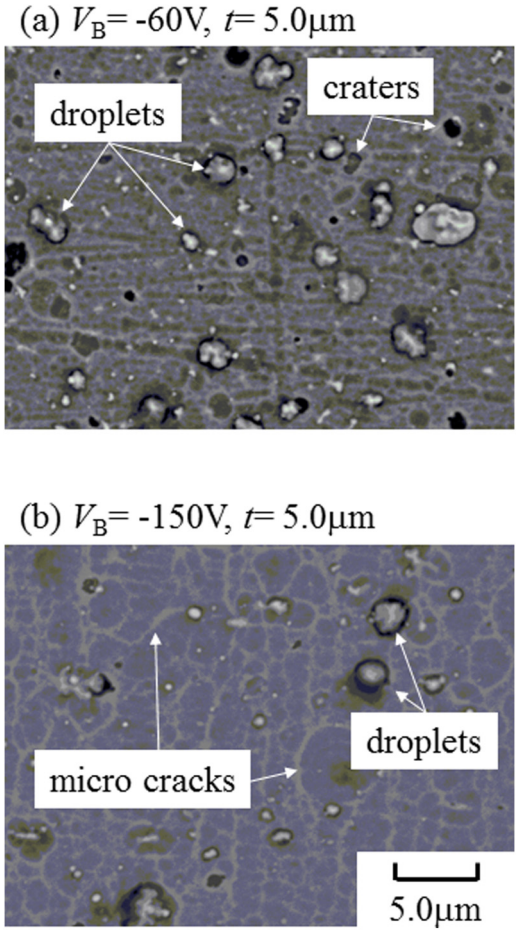

FIG. 5. SEM images of the surface of the 5 μm-thick CrN coating deposited at (a) $V_B = -60$ V and (b) $V_B = -150$ V.

were many microcracks in the surface of the CrN coating that had been deposited when $V_B = -150$ V, $t = 5\,\mu$m shown in Fig. 5(b). Therefore, the large compressive residual stress was released by these cracks.

IV. SUMMARY AND CONCLUSION

The crystal orientation and the residual stresses in hard CrN coatings deposited on the soft aluminum alloy substrate at various bias voltages (V_B) and various coating thicknesses (t) were measured via x-ray diffraction. The results obtained were as follows:

(1) The crystal structure of the CrN coatings deposited at low V_B was of the same perfectly random orientation as the CrN powder, whereas the CrN coatings deposited at high V_B had a mixed structure of random and {110} oriented crystals.
(2) The residual stresses in the Al alloy substrate were almost zero, irrespective of the deposition conditions. The very large compressive residual stress occurred in all CrN coatings.
(3) The 2θ-$\sin^2\psi$ diagram for the coating deposited at $V_B = -60$ V, $t = 2\,\mu$m was an upward convex curve due to the large compressive residual stress only in the

vicinity of the interface with the substrate. Conversely, the 2θ-$\sin^2\psi$ diagram for the coating deposited at high V_B was a downward convex curve due to the large compressive residual stress only in the coating surface.

(4) Many microcracks occurred in the surface of the CrN coating deposited at a high V_B of -150 V and thickness of 5 μm.

ACKNOWLEDGMENTS

The authors are grateful to the contributions of all the students, including Satoshi Nakai, who were involved in the sample preparation. The authors also would like to thank Enago (www.enago.jp) for the English language review.

[1]A. Kondo, T. Oogami, K. Sato, and Y. Tanaka, Surf. Coat. Technol. **177–178**, 238 (2004).
[2]Y. Kong, X. Tian, C. Gong, and P. K. Chu, Surf. Coat. Technol. **344**, 204 (2018).
[3]A. Lousa, J. Romero, E. Martı´nez, J. Esteve, F. Montalà, and L. Carreras, Surf. Coat. Technol. **146–147**, 268 (2001).
[4]E. Broszeit, C. Friedrich, and G. Berg, Surf. Coat. Technol. **115**, 9 (1999).
[5]C. Öner, H. Hazar, and M. Nursoy, Mater. Des. **30**, 914 (2009).
[6]N. Schönberg, Acta Chem. Scand. **8**, 213 (1954).
[7]The Society of Materials Science, JSMS-SD-10-05, 2005.
[8]E. Kröner, Z. Phys. **151**, 504 (1958).
[9]M. Birkholz, *Thin Film Analysis by X-ray Scattering* (Wiley-VCH, Weinheim, 2005), p. 259.
[10]B. D. Cullity and S. R. Stock, *Element of X-ray Diffraction*, 3rd ed. (Prentice Hall, Englewood Cliffs, NJ, 2001), p. 630, Appendix 8.
[11]C. A. Davis, Thin Solid Films **226**, 30 (1993).
[12]P. J. Martin, A. Bendavid, T. J. Kinder, and L. Wielunski, Surf. Coat. Technol. **86–87**, 271 (1996).